Journal of Theoretical and Applied Mechanics, Sofia, Vol. 47 No. 2 (2017) pp. 61-82

FLUID MECHANICS

THEORETICAL EXPLORATION OF EXPONENTIAL HEAT SOURCE AND THERMAL STRATIFICATION EFFECTS ON THE MOTION OF 3-DIMENSIONAL FLOW OF CASSON FLUID OVER A LOW HEAT ENERGY SURFACE AT INITIAL UNSTEADY STAGE

N. SANDEEP[1], I.L. ANIMASAUN[2*]

[1]*Department of Mathematics, VIT University, Vellore-632014, India*
[2]*Department of Mathematical Sciences, Federal University of Technology, Akure, Ondo State, Nigeria*

[Received 20 March 2017. Accepted 26 June 2017]

ABSTRACT: Within the last few decades, experts and scientists dealing with the flow of non-Newtonian fluids (most especially Casson fluid) have confirmed the existence of such flow on a stretchable surface with low heat energy (i.e. absolute zero of temperature). This article presents the motion of a three-dimensional of such fluid. Influence of uniform space dependent internal heat source on the intermolecular forces holding the molecules of Casson fluid is investigated. It is assumed that the stagnation flow was induced by an external force (pressure gradient) together with impulsive. Based on these assumptions, variable thermophysical properties are most suitable; hence modified kinematic viscosity model is presented. The system of governing equations of 3-dimensional unsteady Casson fluid was non-dimensionalized using suitable similarity transformation which unravels the behavior of the flow at full fledge short period. The numerical solution of the corresponding boundary value problem (ODE) was obtained using Runge-Kutta fourth order along with shooting technique. The intermolecular forces holding the molecules of Casson fluid flow in both horizontal directions when magnitude of velocity ratio parameters are greater than unity breaks continuously with an increase in Casson parameter and this leads to an increase in velocity profiles in both directions.

KEY WORDS: Stagnation flow, Impulsive, Intermolecular forces, Casson fluid, Variable plastic dynamic viscosity.

1. INTRODUCTION

The study of fluid mechanics can be referred to as motion of liquid or gasses subjected to an unbalanced forces or stresses such that the motion continues as long as unbalanced forces are applied. This body of knowledge has helped engineers, scientists and physicists to synthesize the transport phenomena of some fluids and this has

*Corresponding author e-mail: anizakph2007@gmail.com

drastically increased efficiency. The understanding of the effect(s) of thermal stratification on the intermolecular forces holding the molecules of non-Newtonian fluid flow with yield stress over a surface at absolute zero can be described as an open question. Scientifically, an answer to such open question may start by explaining the relationship between temperature, kinematic viscosity and a set of repulsive/attractive forces which tends to occur between the molecules of the fluid. Basically, the motion of Casson fluid is based on all these facts. As fluid flows over either a vertical or horizontal surface, Ludwig Prandtl reported the formation of the boundary layer and clarified the discrepancy known as "D'Alembert's paradox"; see Anderson [1], Arakeri and Shankar [2]. Prandtl reported that the viscous effects can never be neglected no matter how small the magnitude of viscosity. Since the presentation of Ludwig Prandtl many researchers have considered the idea of Casson [3] to explain the motion and boundary layer analysis of Casson fluid flow on different surfaces because of its increasing applications in the industry and engineering processes. Pop et al. [4] reported the flow of Casson fluid in the region of stagnation point towards a stretching sheet and analyzed the heat transfer characteristics. Description of non-Newtonian Casson fluid flow with thermophoresis (particle deposition) on free convective heat and mass transfer of non-Darcian flow has been reported by Animasaun [5]. Recently, heat and mass transfer behavior of Casson fluid past an exponentially permeable stretching surface in the presence of thermal radiation has been discussed by Sandeep *et al.* [6]. It was reported that an increase in the magnitude of exponential parameter and heat source parameter enhances the heat transfer rate. Also remarked that the temperature profiles of the non-Newtonian Casson fluid effectively enhances compared with the temperature profiles of a Newtonian fluid. Recently, this attracted Animasaun *et al.* [7] to deliberate on mass transfer during the three-dimensional Casson fluid flow towards a stagnation-point and a surface on which the heat energy falls at lower limit of thermodynamic temperature scale in the presence of cross diffusion. It is observed that Nusselt number decreases significantly with Dufour number at a constant value of Soret number.

In many investigations on fluid flow, researchers have thoroughly investigated a case in which the temperature of the horizontal wall is of higher magnitude than that of free stream temperature. Likewise, there exist some cases in which the temperature of the wall is lesser than that of free stream. Typical example is the fluid flow over a melting surface as reported by Bachok et al. [8] and Kọríkọ *et al.* [9]. This contribution to the body of knowledge attracted Bamisaye et al. [10] to establish the influences of internal heat source and melting surface on the flow of a non-Newtonian fluid (micropolar) when the magnetic-Reynold number of the flow is substantial. It was shown that the micro-rotation and induced magnetic field profiles increase with an increase in the melting. As we are standing on the floor (on planet earth), it may

be realistic and valid to assume that the floor is at absolute zero of temperature (i.e. over a surface in which its heat energy falls at lower limit of the thermodynamic temperature scale). This often results in vertical density variations which is of great importance in industry due to its vast application in the industry. Dake and Harleman [11] extensively discussed the distribution of temperature across a deep lake and further explained the applications of thermal stratification in real life situation. This new idea has been properly considered in Adegbie et al. [12] and reported that it is possible to investigate the effect of temperature on the viscosity of upper-convected Maxwell fluid within thin boundary layer. The effect of temperature due to thermal stratification on layer of fluid next to the melting wall was investigated by Omowaye and Animasaun [13]. In order to choose the proper domain of the flow which is relevant to the real life applications Wang [14] considered a steady three-dimensional flow due to a stretching flat plate and studied only the velocity field. Nath et al. [15] extended the study and investigated unsteady boundary-layer equations governing the flow together with the heat and diffusion transport. Nadeem et al. [16] deliberated on magnetohydrodynamic (MHD) three-dimensional Casson fluid flow past a porous linear stretching sheet and assumed that the horizontal sheet is stretched with two different linear velocities along the plane.

The word "*impulsive*" was used to describe fluid flow by Sir George Stokes; for details, see 47th point in Stoke [17]. Thereafter, series of investigations have been carried out towards the understanding of the dynamics of impulsive induced fluid flow. Williams and Rhyne [18] argued extensively that the viscous flow within the boundary layer develops slowly, reaching a fully develop steady flow only after some period of time. The boundary layer development occurs in two stages (at small time and at large time). It was reported that for small time the fluid flow is dominated by the viscous and pressure gradient forces and the unsteady acceleration. For large time the fluid flow is dominated by the viscous forces, the pressure gradient and the convective acceleration. This led Sandeep and Sugunamma [19] to investigate and report the motion of an unsteady hydromagnetic free convection and radiative heat transfer along a vertical surface due to impulsive. Recently, Motsa and Animasaun [20,21] to deliberate on the motion of unsteady gravity-induced nanofluid flow containing gyrotactic micro-organisms along downward vertical convectively heated surface and vertical surface due to impulsive. In all the above studies, little or no attention has been given to investigate an unsteady three-dimensional boundary layer flow of a Casson fluid over a horizontal surface at absolute zero. In this study, impulsive together with dual stretching of fluid layers adjacent to the wall at both ends are adapted to induce stagnation Casson fluid flow at the stagnation point ($x = 0, y = 0, z = 0$).

The Casson fluid flow along the horizontal surface at absolute zero subject to significant thermal stratification at free stream is theoretically investigated. Another

objective of this study is to investigate full fledge unsteady three-dimensional stagnation Casson fluid flow due to impulsive and dual stretching of fluid layers at the wall and at free stream. This article presents a modified space dependent internal heat source suitable to model the heat distribution in the fluid flow over a surface at absolute zero subject to thermal and solutal stratification. The corresponding effect/influence of temperature on plastic dynamic viscosity and thermal conductivity of Casson fluid is considered. This can be traced to the fact that when the intermolecular forces holding the molecules of Casson fluid are strong, there may be a larger viscosity. Hence, this article proposed a suitable kinematic viscosity which models the physical configuration of the flow. Due to the nature of the Casson fluid flow (i.e. over a surface at absolute zero and subject to thermal stratification), this study presents the effects of temperature on the intermolecular forces, viscosity and velocity profiles in $x-$directions and also in $y-$directions. The knowledge will be useful in paint industry and syrup pharmaceutical industry. In this article, we presents the mathematical formulation of the problem in Section 2. The numerical solution of the dimensionless equations is presented in Section 3. In Section 4 the results and discussions are explained and we presents the conclusions based on the findings in Section 5.

2. MATHEMATICAL FORMULATION

The flow of two-dimensional, incompressible Casson fluid with variable plastic dynamic viscosity and thermal conductivity along a surface at absolute zero is considered. The flow under consideration is assumed to occupy the domain $0 \leq z < \infty$ as shown in Fig. 1. It is assumed that the temperature of the horizontal surface T_a and at the free stream T_∞ satisfies the condition $T_a < T_\infty$.

As shown in Fig. 1, $x-$axis and $y-$axis are taken along the horizontal surface while $z-$axis is taken as normal to the surface. It is assumed that the velocity of the external flow at $y = 0$ as $z \to \infty$ is $u_\infty = ex$ while the velocity of the external flow at $x = 0$ as $z \to \infty$ is $v_\infty = dy$. The velocity of the stretching horizontal surface along $x-$direction is $u_w = ax$ while velocity of the stretching surface along $y-$direction is $v_w = by$. In this study, "a", "e" and "d" are positive constants while "a" corresponds to the stretching rate of horizontal surface in both directions. The variables "x" and "y" measures the distance along the horizontal surface in $x-$ and $y-$direction respectively. In addition, "e" and "d" corresponds to stretching rate of the layer of Casson fluid at free stream along $x-$direction and $y-$direction respectively. Firstly, two equal and opposite forces are introduced along $x-$axis and $y-$axis. Likewise, another two equal and opposite forces are introduced along $x-$axis and $y-$axis few distance above the wall (i.e. above the domain $0 \leq z < \infty$) keeping the origin fixed at $z = 0$. Initially, at $t \leq 0$ the surface and the adjacent Casson fluid are at the same

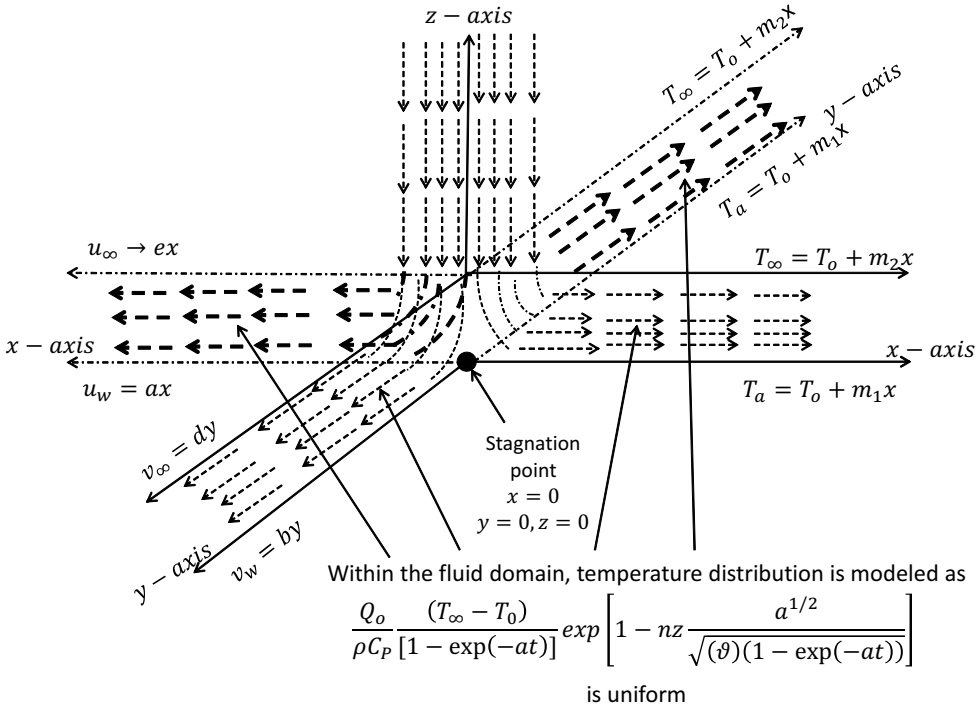

Fig. 1. Physical configuration of the flow.

absolute temperature (T_a) and concentration (C_a); all in a stationary condition. At $t > 0$, the layers of Casson fluid at the free stream is given an impulsive motion in the horizontal direction with respective velocity as stated earlier. The absolute temperature and concentration at the free stream are raised from T_a to T_∞ and C_a to C_∞ respectively. This induce the stagnated Casson fluid to flow in $x-$ and $y-$directions. In this study, we shall consider a case in which the external force associated with stagnation flow complemented impulsive; hence these two forces induces the fluid to flow in $x-$direction and $y-$direction. Using boundary layer approximations (scaling analysis and order of magnitude), the governing equations for three-dimensional fluid are

$$\frac{\partial u}{\partial t} + u\frac{\partial u}{\partial x} + v\frac{\partial u}{\partial y} + w\frac{\partial u}{\partial z} = -\frac{1}{\rho}\frac{\partial p}{\partial x} + \frac{\mu_b}{\rho}\frac{\partial^2 u}{\partial z^2}, \tag{1}$$

$$\frac{\partial v}{\partial t} + u\frac{\partial v}{\partial x} + v\frac{\partial v}{\partial y} + w\frac{\partial v}{\partial z} = -\frac{1}{\rho}\frac{\partial p}{\partial y} + \frac{\mu_b}{\rho}\frac{\partial^2 v}{\partial z^2}. \tag{2}$$

Following the rheological equation by Hayat [22] and Mukhopadhyay [23] for an

isotropic and incompressible flow of a Casson fluid as

$$\tau_{ij} = \left(\mu_b + \frac{P_y}{\sqrt{2\pi}}\right) 2e_{ij} \quad \text{when} \quad \pi > \pi_c, \tag{3}$$

$$\tau_{ij} = \left(\mu_b + \frac{P_y}{\sqrt{2\pi_c}}\right) 2e_{ij} \quad \text{when} \quad \pi < \pi_c, \tag{4}$$

where the yield stress of the Casson fluid denoted by P_y is defined as

$$P_y = \frac{\mu_b \sqrt{2\pi}}{\beta}. \tag{5}$$

Recently, Adebile *et al.* [24] reported that when internal heat source is significant in the fluid domain, the classical kinematic viscosity may not be suitable and hence presented the kinematics viscosity of Casson fluid as a function depending on temperature dependent plastic dynamic viscosity of the non-Newtonian fluid, density of Casson fluid and Casson parameter. Following the explanation and the definition of viscosity given by Sir Isaac Newton in Batchelor [25] together with the context of Eqs. (3)–(5), kinematic viscosity suitable for Casson fluid is of the form

$$\vartheta = \frac{\mu_b(T)}{\rho}\left(1 + \frac{1}{\beta}\right). \tag{6}$$

The impulsive is applied on fluid layer at free stream, this leads to a difference in force which result in an acceleration of the stagnated Casson fluid over a surface at absolute zero. The Bernoulli equation for the free stream flow just above the boundary layer where there is no viscous shear can be differentiated and used to account for the acceleration of external flow along $x-$direction and $y-$direction as

$$-\frac{1}{\rho}\frac{\partial p}{\partial x} = u_\infty \frac{du_\infty}{dx}, \qquad -\frac{1}{\rho}\frac{\partial p}{\partial y} = v_\infty \frac{dv_\infty}{dy}. \tag{7}$$

Substituting Eqs. (7) into Eq. (1) and Eq. (2), then using boundary layer approximations (scaling analysis and order of magnitude), the new kinematic viscosity Eqs. (6), the conservations of total mass and modified momentum equations (in which temperature dependent plastic dynamic viscosity of the non-Newtonian fluid is considered) of 3-dimensional Casson fluid flow are of the form

$$\frac{\partial u}{\partial x} + \frac{\partial v}{\partial y} + \frac{\partial w}{\partial z} = 0, \tag{8}$$

$$\frac{\partial u}{\partial t} + u\frac{\partial u}{\partial x} + v\frac{\partial u}{\partial y} + w\frac{\partial u}{\partial z} = u_\infty \frac{du_\infty}{dx} + \frac{1}{\rho}\left(1 + \frac{1}{\beta}\right)\frac{\partial}{\partial z}\left(\mu_b(T)\frac{\partial u}{\partial z}\right), \tag{9}$$

$$\frac{\partial v}{\partial t}+u\frac{\partial v}{\partial x}+v\frac{\partial v}{\partial y}+w\frac{\partial v}{\partial z}=v_{\infty}\frac{dv_{\infty}}{dy}+\frac{1}{\rho}\left(1+\frac{1}{\beta}\right)\frac{\partial}{\partial z}\left(\mu_b(T)\frac{\partial v}{\partial z}\right), \tag{10}$$

The above governing equations are subject to the following boundary conditions

$$t\leq 0: \quad u=0, \quad v=0, \quad T=T_a, \quad C=C_a, \ \forall \ z \tag{11}$$

Boundary conditions of velocity along $x-$direction in the absence of suction/injection when $t>0$

$$u=u_w(=ax), \ \ w=w_w\left(=-c\sqrt{\xi a\vartheta}\int\frac{v}{ay}\partial\eta\right), \quad \text{at} \ \ z=0 \ \ \text{and} \ \ y=0.$$

$$u\to u_{\infty}(=ex) \ \ \text{as} \ \ z\to\infty \ \ \text{and} \ \ y=0. \tag{12}$$

Boundary conditions of velocity along $y-$direction in the absence of suction/injection when $t>0$

$$v=v_w(=by), \quad w=w_w\left(=-\sqrt{\xi a\vartheta}\int\frac{u}{ax}\partial\eta\right), \quad \text{at} \quad z=0 \quad \text{and} \quad x=0.$$

$$v\to v_{\infty}(=dy) \quad \text{as} \quad z\to\infty \quad \text{and} \quad x=0. \tag{13}$$

In this research, it is assumed that the distribution of temperature in Casson fluid as it flows along $x-$direction and also along $y-$direction is uniform. This can be traced to the fact that the internal heat source distributes uniform temperature along the two directions. It is worth mentioning that in this study, the horizontal surface that we are considering is situated in hot environment ($T_a<T_{\infty}$). In addition, it is of important to note that the stratification of temperature also influences the concentration at the wall and also at the free stream. In view of this, the influence is properly considered. In this study, it is very important to remark that $C_a<C_{\infty}$. In this study, the exponential heat source is adopted to account for internal distribution of temperature in energy equation. This concept can be traced to the idea of Crepeau and Clarksean [26], Salem and El-Aziz [27]. It is very important to remark that the space dependent internal heat source is modeled such that its existence at initial unsteady stage following [18] is significant. The energy and concentration equations can be written as

$$\begin{aligned}\frac{\partial T}{\partial t}+u\frac{\partial T}{\partial x}+v\frac{\partial T}{\partial y}+w\frac{\partial T}{\partial z}\\ =\frac{1}{\rho C_p}\frac{\partial}{\partial z}\left(\kappa_b(T)\frac{\partial T}{\partial z}\right)+\frac{Q_o}{\rho C_p}\frac{(T_{\infty}-T_o)}{[1-\exp(-at)]}exp\left[1-nz\sqrt{\frac{a}{\vartheta\xi}}\right],\end{aligned} \tag{14}$$

$$\frac{\partial C}{\partial t} + u\frac{\partial C}{\partial x} + v\frac{\partial C}{\partial y} + w\frac{\partial C}{\partial z} = D_m \frac{\partial^2 C}{\partial z^2}. \tag{15}$$

Considering both thermal and solutal stratification, boundary condition of temperature and concentration are

$$t \leq 0 : \qquad T = T_a \;\; C = C_a \;\; \forall \;\; z$$

$$t > 0 : \;\; T = T_a (= T_o + m_1 x), \quad C = C_a (C_o + m_3 x) \;\; \text{at} \;\; z = 0. \tag{16}$$

$$t > 0 : \;\; T \to T_\infty (= T_o + m_2 x), \quad C \to C_\infty (C_o + m_4 x) \;\; \text{as} \;\; z \to \infty. \tag{17}$$

In order to account for the variation in thermo-physical properties of Casson fluid as it flows past a horizontal surface, it is valid to consider the modified mathematical model of temperature dependent viscosity model reported in Animasaun [28] together with the modified mathematical model of temperature dependent thermal conductivity model in Ref. [13], similarity variables of temperature and concentration as

$$\begin{gathered} \mu_b(T) = \mu_b^*[\varsigma + j_1(T_\infty - T)], \quad \kappa_b(T) = \kappa_b^*[\varsigma + j_2(T - T_a)], \\ \theta(\eta, \xi) = \frac{T - T_a}{T_\infty - T_o}, \quad \phi(\eta, \xi) = \frac{C - C_a}{C_\infty - C_o}. \end{gathered} \tag{18}$$

These modified models in Eq. (18) are considered based on the fact that in this study $T_a < T_\infty$. Considering the relationship between plastic dynamic viscosity, exponentially internal heat source and free stream temperature of Casson fluid as stated in the first term of Eq. (18) together with dimensionless temperature $\theta(\eta, \xi)$ as defined in Eq. (18), $1 - \theta(\eta, \xi)$ can be easily obtained. Then substituting $T_a = T_o + m_1 x$,

$$T_\infty - T = (1 - \theta(\eta, \xi)) \times ([T_\infty - T_o] - m_1 x) \tag{19}$$

The kinematic viscosity of Casson fluid Eq. (6) as it flows over a surface at absolute zero situated in hot environment together with thermal stratification is proposed as

$$\vartheta = \left(1 + \frac{1}{\beta}\right) \frac{\mu_b^*[\varsigma + j_1(1 - \theta)[T_\infty - T_o] - j_1 m_1 x]}{\rho} \tag{20}$$

Using thermal and solutal stratification models defined in Eq. (16) and Eq. (17), it is easy to deduce that

$$j_1(T_a - T_o) = j_1 m_1 x, \;\; \textit{and} \;\; j_1(T_\infty - T_o) = j_1 m_2 x. \tag{21}$$

T_o and C_o are known as reference temperature and concentration respectively. It is worth noticing from Eq. (21) that there exist two differences in temperature due to stratification. The two different temperature dependent viscosity parameters can be obtained, and these are of the form

$$\begin{aligned} &\omega_\infty = j_1(T_\infty - T_o),\ \omega_a = j_1(T_a - T_o) = \omega_\infty S_t, \\ &S_t = \frac{m_1}{m_2} = \frac{\omega_a}{\omega_\infty},\ S_{sol} = \frac{m_3}{m_4} \end{aligned} \tag{22}$$

Upon substituting Eq. (16) – Eq. (22) into Eq. (9) and Eq. (10) we obtained the transformed governing equations

$$\begin{aligned} &\frac{\partial u}{\partial t} + u\frac{\partial u}{\partial x} + v\frac{\partial u}{\partial y} + w\frac{\partial u}{\partial z} = e^2 \\ &\quad + \vartheta^*[\varsigma - \omega_\infty - \theta\omega_\infty - \omega_\infty S_t]\Big(1 + \frac{1}{\beta}\Big)\frac{\partial^2 u}{\partial z^2} - \Big(1 + \frac{1}{\beta}\Big)\frac{\partial u}{\partial z}\vartheta^*\omega_\infty\frac{\partial \theta}{\partial z}, \end{aligned} \tag{23}$$

$$\begin{aligned} &\frac{\partial v}{\partial t} + u\frac{\partial v}{\partial x} + v\frac{\partial v}{\partial y} + w\frac{\partial v}{\partial z} = d^2 \\ &\quad + \vartheta^*[\varsigma - \omega_\infty - \theta\omega_\infty - \omega_\infty S_t]\Big(1 + \frac{1}{\beta}\Big)\frac{\partial^2 v}{\partial z^2} - \Big(1 + \frac{1}{\beta}\Big)\frac{\partial v}{\partial z}\vartheta^*\omega_\infty\frac{\partial \theta}{\partial z}, \end{aligned} \tag{24}$$

Also, substituting second and third terms of Eq. (18) into Eq. (14)

$$\eta = z\sqrt{\frac{a}{\vartheta\xi}}, \quad \xi = 1 - \exp(-\chi), \quad \chi = at. \tag{25}$$

Transformed energy equation is

$$\begin{aligned} &\frac{\partial T}{\partial t} + u\frac{\partial T}{\partial x} + v\frac{\partial T}{\partial y} + w\frac{\partial T}{\partial z} = \frac{\kappa_b^*[\varsigma + \varepsilon\theta]}{\rho C_p}m_2 x\frac{\partial^2\theta}{\partial\eta^2}\frac{a}{\vartheta\xi} \\ &\qquad + \frac{\kappa_b^* m_2 x}{\rho C_p}\varepsilon\frac{\partial\theta}{\partial z}\frac{\partial\theta}{\partial z}\frac{a}{\vartheta\xi} + \frac{Q_o}{\rho C_p}\frac{m_2 x}{\xi}\exp\left[1 - nz\sqrt{\frac{a}{\vartheta\xi}}\right], \end{aligned} \tag{26}$$

The final step of non-dimensionalization is accomplished by using the following similarity variables extracted from [29]

$$u = ax\frac{\partial f(\eta,\xi)}{\partial\eta}, \quad v = ay\frac{\partial g(\eta,\xi)}{\partial\eta}, \quad w = -\sqrt{\xi a\vartheta}[f(\eta,\xi) + cg(\eta,\xi)]. \tag{27}$$

In order to investigate the initial unsteady stage only, upon substituting Eq. (22), Eq. (25) and Eq. (27) into Eq. (8), Eq. (23), Eq. (24), Eq. (26) and Eq. (15), the corresponding dimensionless partial governing equations are reduced to coupled system of ordinary differential equations by setting $\xi = 0$

$$[\varsigma - \omega_\infty - \theta\omega_\infty - \omega_\infty S_t]\left(1+\frac{1}{\beta}\right)\frac{d^3f}{d\eta^3} - \left(1+\frac{1}{\beta}\right)\omega_\infty \frac{d^2f}{d\eta^2}\frac{d\theta}{d\eta} + \frac{\eta}{2}\frac{d^2f}{d\eta^2} = 0, \tag{28}$$

$$[\varsigma - \omega_\infty - \theta\omega_\infty - \omega_\infty S_t]\left(1+\frac{1}{\beta}\right)\frac{d^3g}{d\eta^3} - \left(1+\frac{1}{\beta}\right)\omega_\infty \frac{d^2g}{d\eta^2}\frac{d\theta}{d\eta} + \frac{\eta}{2}\frac{d^2g}{d\eta^2} = 0, \tag{29}$$

$$[\varsigma + \varepsilon\theta]\frac{d^2\theta}{d\eta^2} + \varepsilon\frac{d\theta}{d\eta}\frac{d\theta}{d\eta} + P_r\frac{\eta}{2}\frac{d\theta}{d\eta} + P_r\gamma exp[1 - n\eta] = 0, \tag{30}$$

$$\frac{d^2\phi}{d\eta^2} + S_c\frac{\eta}{2}\frac{d\phi}{d\eta} = 0. \tag{31}$$

Subject to the following dimensionless boundary equations

$$\begin{aligned} &\frac{df}{d\eta} = 1, \quad f(\eta) = 0, \quad \frac{dg}{d\eta} = \frac{b}{a} = c, \\ &g(\eta) = 0, \quad \theta(\eta) = 0, \quad \phi(\eta) = 0, \quad \text{at} \quad \eta = 0 \end{aligned} \tag{32}$$

$$\begin{aligned} &\frac{df}{d\eta} \to \lambda_1\left(=\frac{e}{a}\right), \quad \frac{dg}{d\eta} \to \lambda_2\left(=\frac{d}{a}\right), \\ &\theta(\eta) \to (1 - S_t), \quad \phi(\eta) \to (1 - S_{sol}) \quad \text{as} \quad \eta \to \infty. \end{aligned} \tag{33}$$

Where, space dependent heat source parameter $\gamma = Q_o/(\rho C_p a)$, Prandtl number $P_r = C_p\mu_b/\kappa_b$ and Schmidt number $S_c = \vartheta/D_m$. The physical quantities of interest in this problem are skin friction coefficients, Nusselt number and Sherwood number. These are defined as

$$\begin{aligned} C_f &= \frac{\vartheta}{a^2x^{3/2}}\left.\frac{\partial u}{\partial z}\right|_{z=0}, \quad C_g = \frac{\vartheta}{a^2x^{3/2}}\left.\frac{\partial v}{\partial z}\right|_{z=0}, \\ Nu &= \frac{-\kappa_b\left.\frac{\partial T}{\partial z}\right|_{z=0}x}{\kappa_b(T_\infty - T_o)}, \quad Sh = \frac{-D_m\left.\frac{\partial C}{\partial z}\right|_{z=0}x}{D_m(C_\infty - C_o)}. \end{aligned} \tag{34}$$

Since the temperature and species distributions are uniform along $x-$ and $y-$directions, Nusselt and Sherwood number are only defined along $x-$direction. Using the transformation variables in Eq. (18), Eq. (25) and Eq. (27) $Re_x = \dfrac{ax}{\vartheta}$ and $Re_y = \dfrac{ay}{\vartheta}$

we obtain the following dimensionless quantities which are proportional to local skin friction coefficient, local heat transfer and local mass transfer

$$
\begin{aligned}
& f''(0,\xi) = \sqrt{\xi} C_f \sqrt{Re_x}, \quad g''(0,\xi) = \sqrt{\xi} C_g \sqrt{Re_y}, \\
& -\theta'(0,\xi) = \frac{\sqrt{\xi}}{\sqrt{xRe_x}} Nu, \quad -\phi'(0,\xi) = \frac{\sqrt{\xi}}{\sqrt{xRe_x}} Sh, \ \ \xi > 0.
\end{aligned} \tag{35}
$$

3. NUMERICAL METHOD OF SOLUTION

Numerical solutions of the ordinary differential Eq. (28) – Eq. (31) subject to boundary conditions Eq. (32) and Eq. (33) are obtained using classical Runge-Kutta method with shooting techniques. The BVP cannot be solved on an infinite interval and it would be impractical to solve it for even a very large finite interval. In this study, the infinite boundary condition at a finite point η at infinity is 9. The set of coupled nonlinear ordinary differential equations along with boundary conditions have been reduced to a system of ten simultaneous equations of first order for ten unknowns following the method of superposition Na [30]. In order to integrate the corresponding IVP the values of $f''(0)$, $g''(0)$, $\theta'(0)$ and $\phi'(0)$ are required, but no such values exist after the non-dimensionalization of the boundary conditions Eq.(32) and Eqs.(33). To resolve this numerically, guessing and Newton-Raphson technique are adopted. The suitable guess values were chosen and then integration was carried out. The Newton-Raphson technique was embedded as root finding of the non-linear equations of the corresponding systems of ten first order ordinary differential equations. At a constant values of λ_1, λ_2, S_t and S_{sol}, the calculated values for $f(\eta)$, $g(\eta)$, $\theta(\eta)$ and $\phi(\eta)$ at $\eta = 9$ are compared with the known boundary conditions in Eq. (33) and the estimated values $f''(0)$, $g''(0)$, $\theta'(0)$ and $\phi'(0)$ are adjusted to give a better approximation of the solution. Series of values for $f''(0)$, $g''(0)$, $\theta'(0)$ and $\phi'(0)$ are considered using step size $\triangle\eta = h = 0.001$. The above procedure is repeated until asymptotically converged results are obtained with tolerance level of 10^{-5}. Finally, fourth-order classical Runge-Kutta scheme is used to solve the ten systems of first order ordinary differential equations subject to conditions stated in Eq. (32) together with the values of $f''(0)$, $g''(0)$, $\theta'(0)$ and $\phi'(0)$ which satisfies the tolerance.

3.1. VERIFICATION OF THE RESULTS

In order to verify the accuracy of the present analysis, the results of Classical Runge-Kutta together with shooting technique have been compared with that of MATLAB package (`bvp4c`) solution for the limiting case when $\omega_\infty = 0.2$, $\varepsilon = \gamma = 0.2$, $n = 3.8$, $\varsigma = 1$, $P_r = 0.71$, $S_c = 0.62$, $c = 0.6$, $\lambda_1 = \lambda_2 = 0.4$ and $S_t = S_{sol} = 0.2$ at various values of β as $\eta \to 9$. The comparison in the above case is found to be in

good agreement, as shown in Table 1. The good agreement is an encouragement for further study of the effects of other parameters on the fluid flow.

Table 1. Comparison of $f''(0)$ and $g''(0)$ using Runge-Kutta with shooting technique and MATLAB package (`bvp4c`)

β	$f''(0)$-RK4SM	$f''(0)$-`bvp4c`	$g''(0)$-RK4SM	$g''(0)$-`bvp4c`
0.2	-0.1229191541	-0.1229191530	-0.0409730513	-0.0409730510
0.4	-0.1618447022	-0.1618447005	-0.0539482340	-0.0539482335
0.6	-0.1859480604	-0.1859480581	-0.0619826868	-0.0619826860
0.8	-0.2027943944	-0.2027943916	-0.0675981314	-0.0675981305

4. Results and Discussion

The numerical computations have been carried out for various values of temperature dependent plastic dynamic viscosity parameters [ω_∞], thermal stratification parameter [S_t], solutal stratification parameter [S_{sol}], temperature dependent thermal conductivity parameter [ε], Prandtl number [P_r], space dependent heat source parameter [γ], intensity of heat distribution on space parameter [n] and Schmidt number [S_c] using numerical scheme discussed in the previous section. In order to illustrate the results graphically, acceptable numerical values are assigned to parameters and solutions were plotted and illustrated in Figs. 2–11. In this theoretical study, either

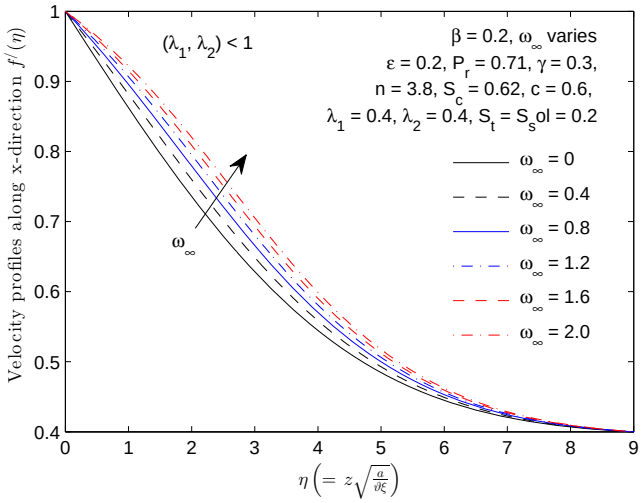

Fig. 2. Effects of temperature dependent variable viscosity parameter ω_∞ on velocity profiles ($x-$direction) [$\lambda_1(=0.4)$ and $\lambda_2(=0.4)$].

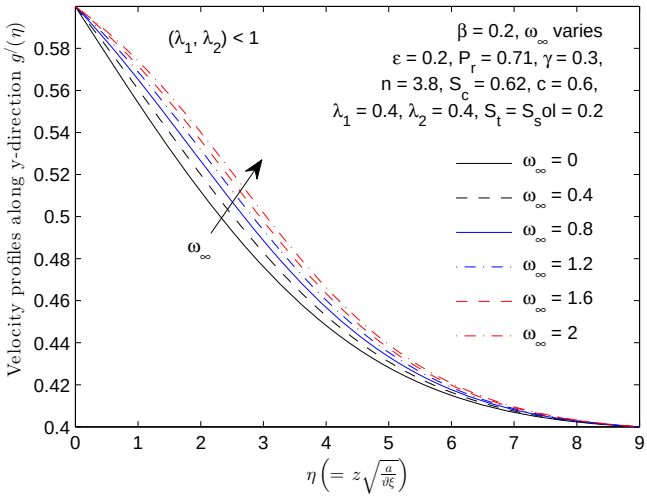

Fig. 3. Effects of temperature dependent variable viscosity parameter ω_∞ on velocity profiles ($y-$direction) [$\lambda_1(=0.4)$ and $\lambda_2(=0.4)$].

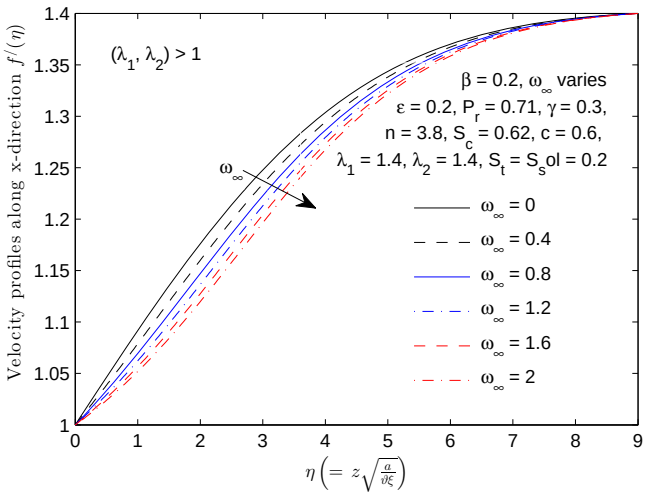

Fig. 4. Effects of temperature dependent variable viscosity parameter ω_∞ on velocity profiles ($x-$direction) [$\lambda_1(=1.4)$ and $\lambda_2(=1.4)$].

increase/decrease in the volume or quality of Casson fluid with an increase in magnitude of ω_∞ and ε have been avoided by setting parameter $\varsigma = 1$. When Casson parameter $\beta(=0.2)$, velocity ratio parameter ($x-$direction) $\lambda_1(=0.4)$, velocity ratio parameter ($y-$direction) $\lambda_2(=0.4)$ at a constant value of temperature dependent

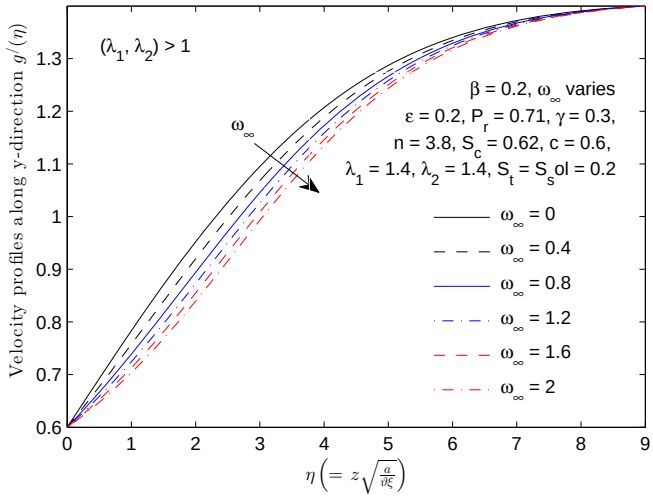

Fig. 5. Effects of temperature dependent variable viscosity parameter ω_∞ on velocity profiles ($y-$direction) [$\lambda_1(=1.4)$ and $\lambda_2(=1.4)$].

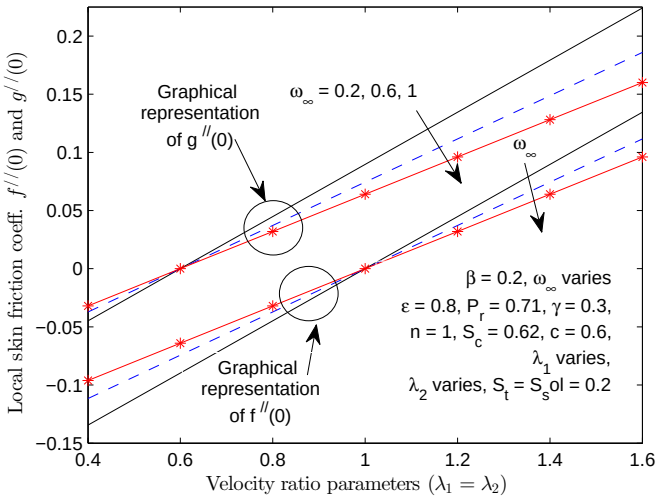

Fig. 6. Variations in $f''(0)$ and $g''(0)$ with (λ_1, λ_2) at different values of ω_∞.

thermal conductivity parameter ($\varepsilon = 0.2$); effects of ω_∞ on the intermolecular forces holding all the molecules of 3-dimensional Casson fluid flow are investigated. It is observed that both velocity profiles $f'(\eta)$ and $g'(\eta)$ increases with an increase in ω_∞ as shown in Fig. 2 and Fig. 3. At a constant reference temperature (T_o), an increase in the magnitude of ω_∞ implies an increase in temperature difference $(T_\infty - T_o)$.

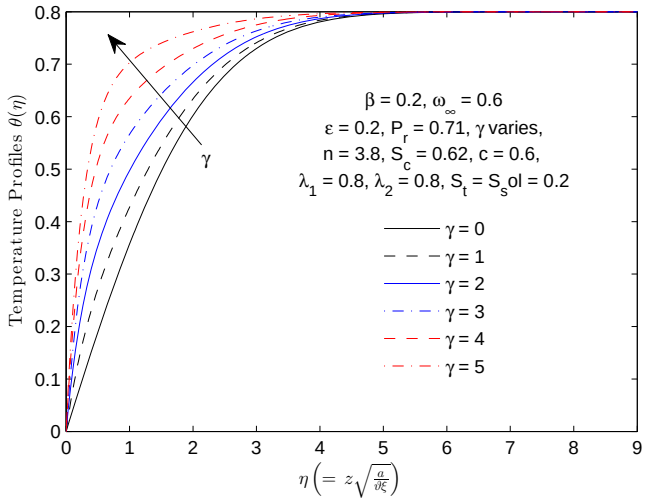

Fig. 7. Effects of γ on temperature profiles.

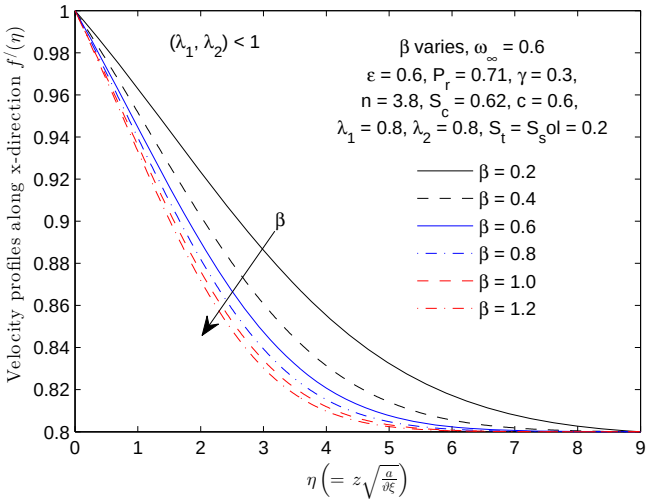

Fig. 8. Velocity profiles ($x-$dir.) for different values of β when $\lambda_1 = \lambda_2 = 0.8$.

It is worth pointing out that T_∞ is the free stream temperature which is strongly associated with thermal stratification parameter S_t. The quantitative increase in the amount of temperature due to an increase in ω_∞ is converted to heat energy and breaks down all the intermolecular forces within the Casson fluid flow. As temperature difference $(T_\infty - T_o)$ increases, the average intermolecular forces decreases and

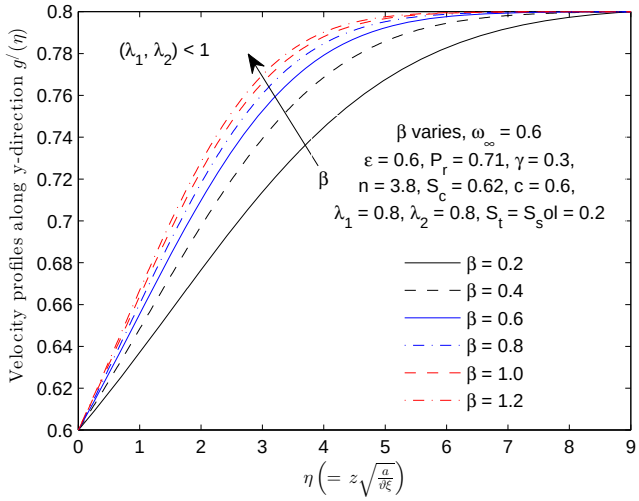

Fig. 9. Velocity profiles ($y-$dir.) for different values of β when $\lambda_1 = \lambda_2 = 0.8$.

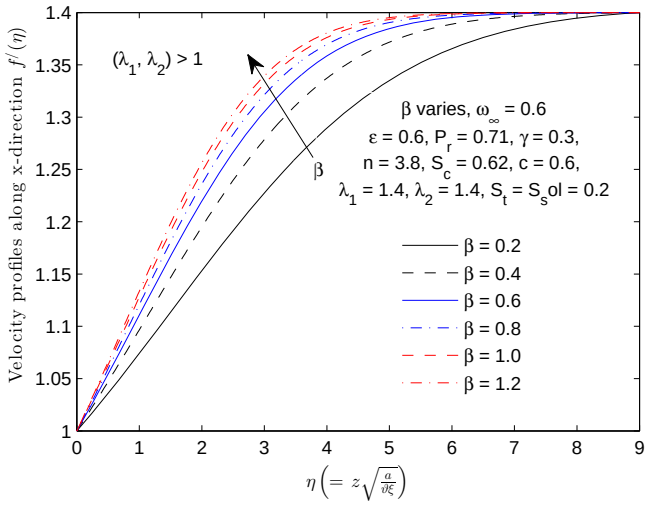

Fig. 10. Effects of Casson parameter β on velocity profiles ($x-$direction) [$\lambda_1(= 1.4)$ and $\lambda_2(= 1.4)$].

the molecules of Casson fluid flow are able to interact in a decreasing manner. In this study, it is observed that the increase in velocities $f'(\eta)$ and $g'(\eta)$ due to increase in ω_∞ are functions depending on ratio parameters λ_1 and λ_2. Using $\lambda_1 = \lambda_2 = 0.4$ either implies stretching rate of the fluid layers at free stream $(e = d = 0.4)$ which is lesser than the rate of stretching of the fluid layers adjacent to the surface at absolute

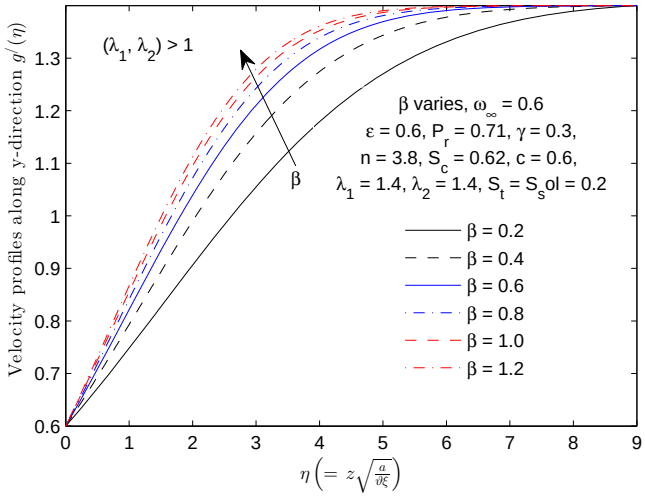

Fig. 11. Effects of Casson parameter β on velocity in $y-$dir. $g'(\eta)$ [$\lambda_1(=1.4)$ and $\lambda_2(=1.4)$].

zero ($a=1$) or stretching of the fluid layers at free stream is unity (i.e. $e=d=1$) which is lesser than the rate of stretching of the fluid layers adjacent to the absolute wall ($a=2.5$). Physically as the magnitude of ω_∞ increases, stretching of fluid layers adjacent to the wall is greater than the stretching of the fluid layers at the free stream. Since the Casson fluid is in contact with the wall, this enhance the reduction in strength of the intermolecular forces holding the molecules of the fluid; and hence explains the increase in $f'(\eta)$ and $g'(\eta)$ with ω_∞ as shown in Fig. 2 and Fig. 3. In addition, the effects of ω_∞ on the velocity functions $f'(\eta)$ and $g'(\eta)$ when $(\lambda_1,\lambda_2)>1$ is investigated. Using $\lambda_1=\lambda_2=1.4$ implies stretching rate of the fluid layers at free stream is 1.4 which is greater in magnitude than the stretching rate of the fluid layers adjacent to the surface at absolute zero ($a=1$) or stretching of the fluid layers at free stream is unity (i.e. $e=d=1$) which is greater than the rate of stretching of the fluid layers adjacent to the surface at absolute zero ($a=0.714$). It is observed in Fig. 4 and Fig. 5 that the influence of excessive stretching at the free stream overpowers the influence of increasing ω_∞. As temperature difference $(T_\infty-T_o)$ increases, the corresponding heat energy actually breaks down all the intermolecular forces but the stretching effect dominates and leads to decrease in $f'(\eta)$ and $g'(\eta)$ with ω_∞. The variations of local skin friction coefficients $f''(0)$ and $g''(0)$ with velocity ratio parameters (λ_1,λ_2) at different values of temperature dependent plastic dynamic viscosity parameters (ω_∞) are shown in Fig. 6. It is observed that the point of intersection in $f''(0)$ is 1 while the point of intersection in $g''(0)$ is 0.6.

Physically, these points are dependent on the stretching rate at the wall which are $f'(\eta = 0) = 1$ and $g'(\eta = 0) = c = 0.6$. It is seen that before the intersection points mentioned above as ω_∞ increases, local skin friction coefficients $f''(0)$ and $g''(0)$ increases significantly along $x-$direction and increases negligibly along $y-$direction respectively. It is worth mentioning that this is the case in which influence of temperature on the intermolecular forces is enhanced by the stretching of the horizontal surface in both directions. Due to the increase in the velocity profiles, the skin friction coefficients increases as well. Reverse is the case when velocity ratio parameters $(\lambda_1, \lambda_2) > 1$. It is observed that local skin friction coefficients $[f''(0),\ g''(0)]$ decreases along $x-$direction and $y-$direction with an increase ω_∞. It is further observed that the nature of heat energy at the surface (wall) which is of absolute zero accounts for the reason why temperature at the wall is zero as shown in Fig. 7. The increase in the magnitude of space dependent internal heat source that exists at initial unsteady stage γ leads to an increase in temperature profiles. Effects of Casson parameter (β) on the velocity functions $f'(\eta)$ and $g'(\eta)$ are shown in Figs. 8–11. When $\lambda_1 = \lambda_2 = 0.8$, it is observed that $f'(\eta)$ decreases with an increase in the magnitude of Casson parameter. An increase in β implies a decrease in yield stress P_y of the Casson fluid; this effect creates resistance in the fluid flow; see Fig. 8. The reverse is the case as shown in Fig. 9. It is observed that stretching of velocity along $y-$direction strongly influences the fluid flow. The increasing effect in velocity profiles $g'(\eta)$ as shown in Fig. 9 can be traced to the boundary condition $[g'(\eta = 0) = c = 0.6] < [g'(\eta \to \infty) = \lambda_2 = 0.8]$. The effect of Casson parameter β on the velocity of 3-dimensional stagnation Casson fluid flow over a surface at absolute zero when velocity ratio parameter $\lambda_1 = \lambda_2 = 1.4$ is illustrated in Fig. 10 and Fig. 11. It is observed that the excessive stretching of Casson fluid at free stream enhance the effects of increasing Casson parameter; a significant increase of $f'(\eta)$ and $g'(\eta)$ within the fluid domain $0 \leq \eta \leq 9$. It is further observed that as $\beta \to \infty$, the characteristics of the non-Newtonian fluid is tending towards that of Newtonian fluid. This leads to a negligibly increase in $f'(\eta)$ and $g'(\eta)$ when β increases from 1.0 to 1.2. Table 2 depicts the influence of modified space dependent internal heat source parameter γ on Nusselt number and Sherwood number. The local heat transfer rate which is proportional to Nusselt number decreases with an increase in the magnitude of γ. A negligible decrease in local mass transfer rate due to an increase in γ is also observed.

5. Conclusion

The similarity solutions of 3-dimensional unsteady Casson fluid flow over a surface at absolute zero subject to thermal and solutal stratification have been investigated. All the necessary conditions are properly considered and incorporated into the gov-

Table 2. Numerical result for different values of Nusselt number and Sherwood number when $\beta = 0.2$, $\omega_\infty = 0.4$, $\varepsilon = 0.2$, $n = 3.8$, $\varsigma = 1$, $P_r = 0.71$, $c = 0.6$, $\lambda_1 = \lambda_2 = 0.4$ and $S_t = S_{sol} = 0.2$ at various values of γ as $\eta \to 40$.

γ	$-\theta'(\eta = 0)$	$-\phi'(\eta = 0)$
0.3	-0.52788898857100	-0.35539466710072
0.5	-0.61904185014703	-0.35539466710072
0.7	-0.71020577456582	-0.35539466710072
0.9	-0.80138418316431	-0.35539467398903

erning equations. The governing (dimensional) partial differential equations are converted into (dimensionless) nonlinear ordinary differential equations by using similarity transformation and solved numerically. The influence of modified space dependent internal heat source on the intermolecular forces which bonds the molecules of Casson fluid is properly investigated. The conclusions are as follows:

1. Increase in temperature dependent plastic dynamic viscosity parameters corresponds to increase and decrease in velocity functions of Casson fluid flow when $(\lambda_1, \lambda_2) < 1$ and $(\lambda_1, \lambda_2) > 1$ respectively. When velocity ratio parameter $c < 1$, local skin friction coefficients $f''(0)$ and $g''(0)$ of Casson fluid flow over a surface at absolute zero decreases with an increase temperature dependent plastic dynamic viscosity parameters when $(\lambda_1, \lambda_2) > 1$ and $(\lambda_1, \lambda_2) > 0.6$ respectively.

2. Velocity ratio parameters (λ_1, λ_2) and influence of the horizontal surface at absolute zero have a significant effect on temperature profiles near the wall. Maximum values of γ leads to high quantity of temperature distribution which consequently corresponds to maximum amount of heat energy within Casson fluid as it flows over a horizontal surface at absolute zero. Casson parameter have the tendency to reduce and increase the velocity along $x-$direction only when velocity ratio parameters $(\lambda_1, \lambda_2) < 1$ and $(\lambda_1, \lambda_2) > 1$ respectively.

REFERENCES

[1] ANDERSON, J. D. Ludwig Prandtl's Boundary Layer. *Physics Today*, **58** (2005), No. **12**, 42-48.

[2] ARAKERI, J. H., P. N. SHANKAR. Ludwig Prandtl and Boundary Layers in Fluid Flow. *Resonance*, **5** (2000), No. **12**, 48-63.

[3] CASSON, N. A Flow Equation for Pigment Oil-Suspensions of the Printing Ink Type. *Rheology of Disperse Systems*, **84** (1959), London, Pergamon Press, 1959.

[4] POP, I., M. MUSTAFA, T. HAYAT, A. HENDI. Stagnation-Point Flow and Heat Transfer of a Casson Fluid towards a Stretching Sheet. *Zeitschrift fur Naturforschung A*, **67** (2012), No. **1-2**, 70-76.

[5] ANIMASAN, I. L. Effects of Thermophoresis, Variable Viscosity and Thermal Conductivity on Free Convective Heat and Mass Transfer of Non-Darcian MHD Dissipative Casson Fluid Flow with Suction and n-th Order of Chemical Reaction. *Journal of the Nigerian Mathematical Society*, **34** (2015), No. **1**, 11-31.

[6] RAJU, C. S. K., N. SANDEEP, V. SUGUNAMMA, M. JAYACHANDRA BABU, J. V. RAMANA REDDY. Heat and Mass Transfer in Magnetohydrodynamic Casson Fluid over an Exponentially Permeable Stretching Surface. *Engineering Science and Technology, an International Journal*, **19** (2016), No. **1**, 4552. doi: 10.1016/j.jestch.2015.05.010

[7] SANDEEP, N., O. K. KORIKO, I. L. ANIMASAN. Modified Kinematic Viscosity Model for 3D-Cassonfluidflow within Boundary Layer formed on a Surface at Absolute Zero. *Journal of Molecular Liquids*, **221** (2016), 1197-1206. doi: 10.1016/j.molliq.2016.06.049

[8] BACHOK, N., A. ISHAK, I. POP. Melting Heat Transfer in Boundary Layer Stagnation-point Flow Towards a Stretching/shrinking Sheet. *Physics Letters A*, **374** (2010), No. **40**, 4075-4079. doi: 10.1016/j.physleta.2010.08.032

[9] KỌRÍKỌ, O. K., S. K. ADEGBIE, I. L. ANIMASAN. Melting Heat Transfer Effects on Stagnation Point Flow of Micropolar Fluid with Variable Dynamic Viscosity and Thermal Conductivity at Constant Vortex Viscosity. *Journal of the Nigerian Mathematical Society*, **35** (2015), No. **1**, 34-47. doi: 10.1016/j.jnnms.2015.06.004

[10] KỌRÍKỌ, O. K., A. J. OMOWAYE, I. L., ANIMASAUN, M. E BAMISAYE. Melting Heat Transfer and Induced-Magnetic Field Effects on the Micropolar Fluid Flow towards Stagnation Point: Boundary Layer Analysis. *International Journal of Engineering Research in Africa*, **29** (2017), 10-20. doi:10.4028/www.scientific.net/JERA.29.10

[11] DAKE, J. M. K., D. R. F. HARLEMAN. Thermal Stratification in Lakes: Analytical and Laboratory Studies. *Water Resources Research*, **1** (1969), No. **2**, 484-495.

[12] ADEGBIE, K. S., A. J. OMOWAYE, A. B. DISU, I. L. ANIMASAN. Heat and Mass Transfer of Upper Convected Maxwell Fluid Flow with Variable Thermo-Physical Properties over a Horizontal Melting Surface. *Applied Mathematics*, **6** (2015), 1362-1379.

[13] OMOWAYE, A. J., I. L. ANIMASAN. Upper-Convected Maxwell Fluid Flow with Variable Thermo-Physical Properties over a Melting Surface situated in Hot Environment Subject to Thermal Stratification. *Journal of Applied Fluid Mechanics*, **9** (2016), No. **4**, 1777-1790.

[14] WANG C. Y. The Three-dimensional Flow due to a Stretching Flat Surface. *Physics Fluids*, **27** (1984), 1915-1917.

[15] NATH, G., H. S. TAKHAR. Unsteady, Three-dimensional, Boundary-layer Flow due to a Stretching Surface. *International Journal of Heat and Mass Transfer,* **29** (1986), No. **12**, 1996-1999.

[16] NADEEM, S., U. H. RIZWAN, N. S. AKBAR, Z. H. KHAN. MHD Three Dimensional Casson Fluid Flow Past a Porous Linearly Stretching Sheet. *Alexandria Engineering Journal*, **52** (2013), No. **4**, 577-582.

[17] STOKE, G. G. On the Effect of Internal Friction of Fluids on the Motion of Pendulums. *Trans. Cam. Phil. Soc.,* **9, 8-106** (1851); Mathematics and Physics Papers, Vol. 3, p. 1., Cambridge, Cambridge University Press, **3** (1901), No. **1**., 1-86.

[18] WILLIAMS J. C., T. H. RHYNE. Boundary Layer Development on a Wedge Impulsively Set into Motion. *SIAM Journal of Applied Mathematics*, **38** (1980), 215-224.

[19] SANDEEP, N., V. SUGUNAMMA. Radiation and Inclined Magnetic Field Effects on Unsteady Hydromagnetic Free Convection Flow past an Impulsively Moving Vertical Plate in a Porous Medium. *Journal of Applied Fluid Mechanics,* **7** (2014), No. **2**, 275-286.

[20] MOTSA, S. S., I. L. ANIMASAUN. Paired Quasi-linearization Analysis of Heat Transfer in Unsteady Mixed Convection Nanofluid containing Both Nanoparticles and Gyrotactic Microorganisms due to Impulsive Motion. *Journal of Heat Transfer*, **138** (2016), 114503. doi: 10.1115/1.4034039

[21] MOTSA, S. S., I. L. ANIMASAUN. Unsteady Boundary Layer Flow over a Vertical Surface due to Impulsive and Buoyancy in the Presence of Thermal-Diffusion and Diffusion-Thermo using Bivariate Spectral Relaxation Method. *Journal of Applied Fluid Mechanics*, **9** (2016) No. **5**, 2605-2619.

[22] HAYAT, T., S. A. SHEHZADI, A. ALSAEDI. Soret and Dufour Effects on Magnetohydrodynamic (MHD) Flow of Casson Fluid. *Applied Mathematics Mechanics (English Ed.)*, **33** (2012), No. **10**, 1301-1312.

[23] MUKHOPADHYAY, S. Casson Fluid Flow and Heat Transfer over a Nonlinearly Stretching Surface. *Chinese Physics B*, **22** (2013), No. **7,** 074701.

[24] ADEBILE, E. A., I. L. ANIMASAUN, A. I. FAGBADE. Casson Fluid Flow with Variable Thermo-Physical Property along Exponentially Stretching Sheet with Suction and Exponentially Decaying Internal Heat Generation Using the Homotopy Analysis Method. *Journal of the Nigerian Mathematical Society*, **35** (2016) No. **1**, 1-17. doi: 10.1016/j.jnnms.2015.02.001

[25] BATCHELOR, G. K. An Introduction to Fluid Dynamics, London, Cambridge University Press, 1987.

[26] CREPEAU, J. C., R. CLARKSEAN. Similarity Solutions of Natural Convection with Internal Heat Generation. *Transactions of ASME-Journal of Heat Transfer,* **119** (1997), 184-185.

[27] SALEM, A. M., M. A. EL-AZIZ. MHD-mixed Convection and Mass Transfer from a Vertical Stretching Sheet with Diffusion of Chemically Reactive Species and Space- or Temperature-dependent Heat Source. *Canadian Journal of Physics,* **85** (2007), No. **4**, 359-373.

[28] ANIMASAUN, I. L. Double Diffusive Unsteady Convective Micropolar Flow past a Vertical Porous Plate moving through Binary Mixture using Modified Boussinesq

Approximation. *Ain Shams Engineering Journal*, **7** (2016) No. **2**, 755 -765. doi: 10.1016/j.asej.2015.06.010

[29] TAKHAR, H. S., A. J. CHAMKHA. Unsteady Three-dimensional MHD Boundary-layer Flow due to the Impulsive Motion of a Stretching Surface. *Acta Mechanica*, **146** (2001), No. **1-2**, 59-71.

[30] NA, T. Y. Computational Methods in Engineering Boundary Value Problems, New York, Academic Press, 1979.